

7. Tribological evaluation of PAO 100 oil-based grease using four-ball tribometer

This chapter discusses the grease formulated with PAO 100 as a base oil and 12–lithium hydroxystearate metallic soap as a thickener. The tribological performance of grease was carried out with and without nanoadditives (MWCNTs and LaF₃). The test results unveiled the role of nanoadditives on the lubrication performance of the PAO 100-based grease.

7.1. Characterization of nanoadditives

In this investigation, COOH-functionalized MWCNTs and synthesized oleic acid-modified LaF₃ nanoparticles were employed as additives in PAO 100–based grease. The detailed chemical, structural, and morphological characterizations of COOH-functionalized MWCNTs and oleic acid-modified LaF₃ nanoparticles have been described in **Section 4.1.1** and **Section 6.1**, respectively.

7.2. Physicochemical properties of PAO 100 grease

The synthesis process of PAO 100-based grease is given in preceding Section 3.6. Typical optical images of synthesized PAO 100 greases doped with MWCNTs and LaF₃ nanoadditives are shown in **Figure 7.1**. As the dose of MWCNTs was increased, the colour of the PAO 100 grease gradually darkened (**Figures 7.1(a)-7.1(e)**). In contrast, a minimal change in the colour of the PAO grease was observed when the concentration of LaF₃ was increased (**Figures 7.1(f)-7.1(j)**). The PAO 100 oil-based lithium grease without any nanoadditives is designated as *PAO grease*. The formulated PAO 100 grease samples with varying doses of MWCNTs and LaF₃ nanoparticles (i.e., 0.025–0.15 wt.%) are termed as *MWCNTs grease* and *LaF₃ grease*, respectively. PAO grease was chosen as a reference to compare the physicochemical and tribological properties of MWCNTs and LaF₃ grease

samples. The consistency and drop point of PAO grease with and without nanoadditives were assessed as per ASTM D1403 and D566 standards, respectively. **Figure 7.2** shows the test results of unworked and worked penetrations of PAO grease samples containing various doses of nanoadditives. The worked penetration measurements were taken after shearing of grease via 60 double strokes. The unworked and worked penetration test results indicate that the PAO grease fall in the category of NLGI grade 0. With the addition of MWCNTs and LaF₃ nanoparticles, PAO grease revealed a significant decrease in penetration depth, i.e., an increase in the hardness of PAO grease. It was also observed from **Figure 7.2** that in the case of MWCNTs grease, the worked penetration depth was decreased as the concentration of MWCNTs increased compared to unworked depth penetration. The results revealed that MWCNTs grease samples showed consistency in the range of grade 1- 3 by NLGI. In contrast, all LaF₃ grease samples except 0.025 wt.% LaF₃ grease sample exhibited the increased worked penetration depth compared to unworked penetration depth, and results signify consistency of LaF₃ grease samples in the range of grade 0-2. The variation in unworked and worked penetration implies that the synthesized greases have poor shear stability. PAO grease containing 0.075-0.15 wt.% MWCNTs showed the highest hardness values (lowest penetration depth) and 0.15 wt.% MWCNTs grease is the hardest grease sample.



Figure 7.1: PAO 100 grease having a variable concentration of MWCNTs and LaF₃: (a, f) 0.025 wt.%, (b, g) 0.05 wt.%, (c, h) 0.075 wt.%, (d, i) 0.1 wt.%, and (e, j) 0.15 wt.%

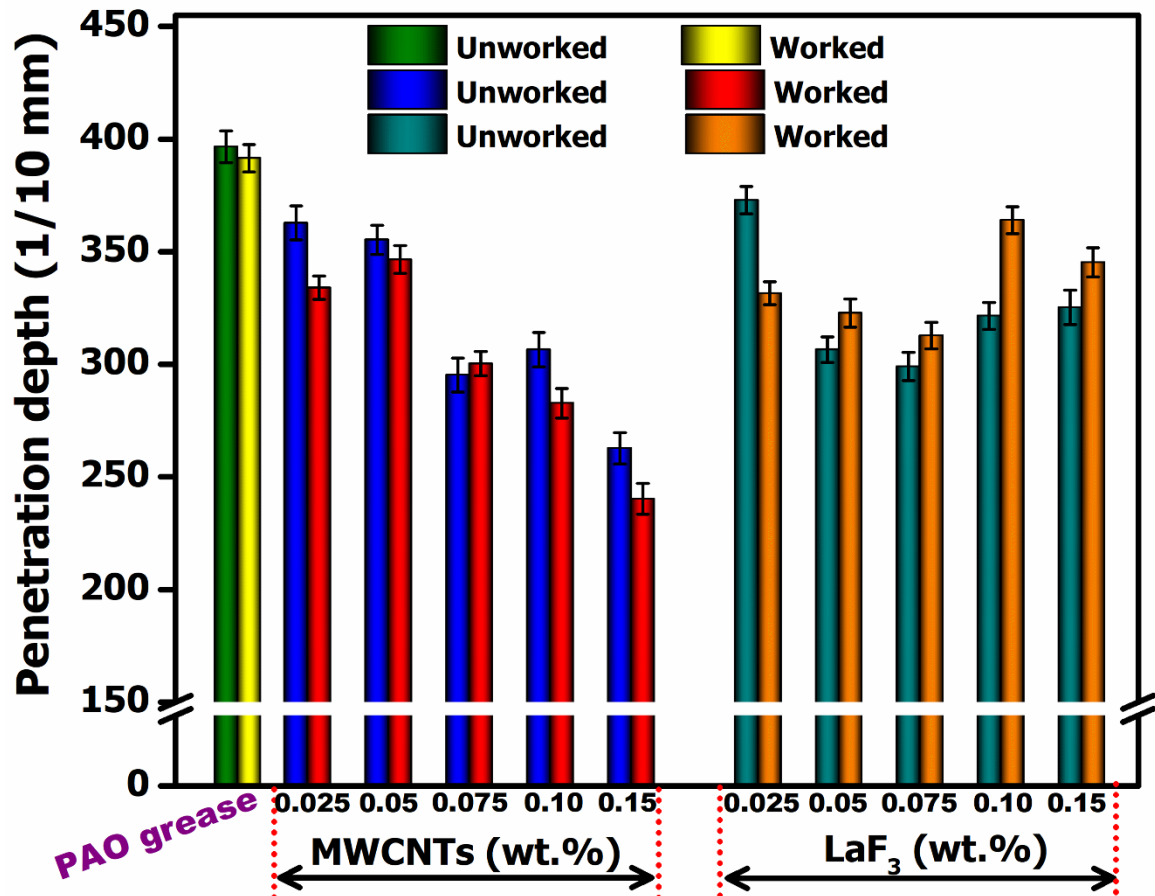


Figure 7.2: Variation in unworked and worked penetration depth of PAO grease with and without nanoadditives

The drop point is also a critical property of lubricating grease that depends on the thickener used in grease formulation. It is a temperature at which the thickener fails to hold base oil inside the fibrous structure of the thickener. It might be possible due to the melting of the thickener or the base oil under the influence of heat transfer so that thin capillary action and surface tension become insufficient to retain the base oil inside the fibrous structure of the thickener. **Figure 7.3** depicts the variation in drop point of PAO grease with varying doses of nanoadditives. The MWCNTs grease and LaF₃ grease samples exhibited augmentation in drop point compared to PAO grease, although the increment in drop point was marginal. The drop point of PAO grease was obtained to be 198 °C, which increased to 211 and 209 °C in the presence of 0.15 wt.% MWCNTs and 0.15 wt.% LaF₃, respectively.

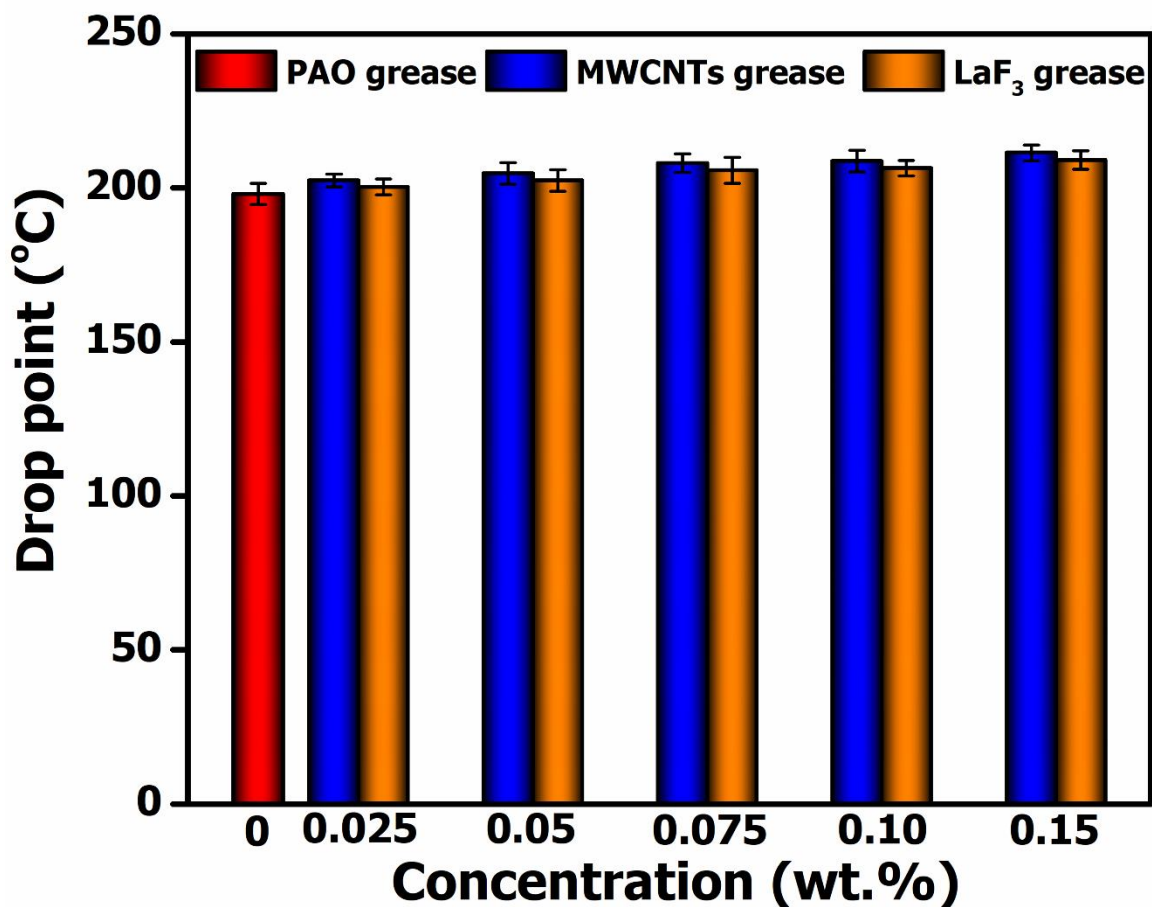


Figure 7.3: Variation in the drop point of PAO grease with and without nanoadditive

7.3. Tribological performance of PAO 100 grease

7.3.1. Antifriction performance of PAO 100 grease

Figure 7.4(a) exhibits the variation in average COF with varying concentrations of nanoadditives. The variation in COF will assist in understanding the efficacy of investigated nanoadditives as a friction modifier during the test duration. The average COF in the case of PAO grease was obtained to be 0.63. With the addition of LaF₃ nanoparticles in PAO grease, the decreasing trend in average COF was observed up to 0.075 wt.% doses of LaF₃. However, it was also noticed that further increasing the dose of LaF₃ beyond 0.075 wt.% in PAO grease resulted in a rise in COF, though it was less than PAO grease. The reason for such behaviour of the additive in PAO grease might be due to additive concentration is too low or too high. Therefore, 0.075 wt.% LaF₃ was found to be the optimum concentration, which exhibited a maximum reduction in COF of approximately 43.5% compared to PAO grease. For MWCNTs grease, minimum average COF was acquired at a dose of 0.05 wt.% of MWCNTs, which was about 14% lower than that of PAO grease. It was also noticed from **Figure 7.4(a)** that the increment in the concentration of MWCNTs beyond 0.05 wt.% demonstrated a gradual increase in average COF, which was higher than PAO grease. The possible reason behind the remarkable rise in the average COF might be the increased hardness of MWCNTs grease samples (or decreased penetration depth), as shown in **Figure 7.2**. The hardness increased dramatically due to a significant increase in surface area/volume ratio of MWCNTs because of aggregation of nanoadditive at a higher concentration which is responsible for thickening the grease samples [172]. The shearing action of MWCNTs grease samples becomes difficult with an increase in hardness during the test. More energy is supposed to be consumed in dealing with this state. As a result, it rises the COF. Overall, LaF₃ grease demonstrated better anti-frictional characteristics compared to MWCNTs grease.

Figure 7.4(b) shows the change in COF with a function of test duration for PAO grease, 0.05 wt.% MWCNTs grease and 0.075 wt.% LaF₃ grease samples. PAO grease exhibited the highest COF (~ 0.079) during the running-in period. As the test progressed, COF continuously decreased till 1500 sec of test duration, followed by fluctuation between 0.069 and 0.056 until the end of the experiment. The friction profile of 0.05wt% MWCNTs grease sample revealed the trend of decrease then remarkable rise, followed by continuous decrease till the end of the test. These transitions in friction profile of 0.05 wt.% MWCNTs grease illustrates that initially, thin layers of PAO grease containing MWCNTs are formed between the interfacial surfaces, leading to a decline in the COF. As the test progresses, these lubricating films are removed due to the build-up frictional force normally exerted by the top rotating steel ball, which causes the increase in COF. After establishing the stable phase (after the running-in period), the MWCNTs arranged themselves in the grooves of asperity and produced low shear strength tribo-film. Consequently, COF was decreased. Moreover, the decreasing trend in the friction profile of MWCNTs grease till the end of experiments indicates that MWCNTs gradually become more involved in lubrication, which enhanced the lubricating effect significantly. It can also be noticed from Figure 7.4(b) that the lowest friction profile with relatively low COF was acquired for 0.075 wt.% LaF₃ grease sample. The decreasing trend in friction profile with test duration signifies continuous activation of LaF₃ at the interface of tribo-pairs, which maintain a stable tribo-film through the friction process that avoids the direct contact of asperities. This phenomenon implies the effective antifriction behaviour of LaF₃ nanoparticles.

During the tribo-tests, friction denotes a loss of energy in the form of heat. Therefore, the amount of energy consumed to overcome friction (i.e., frictional power loss) during tribo-testing was computed using Equation (7.1) [173].

$$P_f = T\omega = \mu Nr\omega \quad (7.1)$$

Where, P_f represents the frictional power loss (MJ), T is frictional torque (Nm), N is total actual contact load on three lower balls (N), ω is the angular velocity (rad/s), μ is the friction coefficient (COF), and r is the friction radius (m).

The calculated frictional power loss for PAO grease incorporating variable concentration of MWCNTs and LaF₃ nanoparticles is summarized in **Table 7.1**. The frictional power loss is directly proportional to the friction coefficient. Therefore, PAO grease containing a higher dose of MWCNTs (0.075-0.15 wt.%) consumed more power to overcome the frictional losses. This power consumption at higher concentrations of MWCNTs was significantly higher compared to PAO grease. However, the addition of 0.05 wt.% MWCNTs in PAO grease revealed the maximum saving in the frictional power loss by ~13.2%. The LaF₃ blended grease at all concentrations showed lower power consumption than MWCNTs blended grease and PAO grease. The optimized dose of LaF₃ (i.e., 0.075 wt.%) reduced the frictional power losses by ~43.5%. These results imply that the inclusion of minute concentrations of both nanoadditives has considerable potential for energy conservation.

7.3.2. Anti-wear performance of PAO 100 grease

Figures 7.4(c)-7.4(d) showed the variation in wear scar diameter (WSD) and mean wear volume (MWV) of PAO grease samples incorporating varied concentrations (0.025-0.15 wt.%) of LaF₃ and MWCNTs nanoadditives. The more prominent WSD (684 μ m) was developed on stationary steel balls when lubricated with PAO grease. It can be noticed from **Figure 7.4(c)** that there was a significant decrease in the WSD of the stationary steel ball when LaF₃ and MWCNTs were used as an additive in PAO grease, but at higher concentrations of LaF₃ and MWCNTs led to an increase in WSD. However, WSD at the higher dose of nanoadditive was lower than that of PAO grease. The LaF₃ grease at all

concentrations except 0.05 wt.% LaF₃ exhibited the lower WSD compared to MWCNTs grease. In contrast, 0.05 wt.% dose of MWCNTs was found to be the optimum concentration in the case of MWCNTs grease samples which produced the lowest WSD (552 μm) with a maximum reduction of approximately ~19%. In the case of LaF₃ grease, the minimum WSD (564 μm) was obtained at 0.075 wt.% concentration of LaF₃, and the maximum reduction in WSD was about 18%. **Figure 7.4(d)** shows the changes in MWV for grease samples having a variable concentration of LaF₃ and MWCNTs. The 0.075 wt.% of LaF₃ grease showed maximum reductions in MWV (~57%), whereas 0.05 wt.% of MWCNTs grease exhibited corresponding higher diminution in MWV (~61%) compared to the PAO grease. It can be observed from **Figures 7.4(c)-7.4(d)** that the changes in the WSD with the addition of nanoadditives were lower than those in MWV, corresponding with the difference between a length and a volume-based approach and demonstrating that MWV is a better comparative parameter in four-ball tests[174]. The results illustrated that both nanoadditives revealed the potential as an anti-wear additive. Although, overall LaF₃ nanoparticles outperformed the MWCNTs. This may be due to the smaller size of LaF₃ nanoparticles compared to MWCNTs. It is commonly understood that the smaller size led to the higher benefits because of the enhanced interaction of smaller particles with metal asperities, resulting in the formation of a thin and beneficial film on the asperities and tribo-surfaces in contacts.

7.3.3. Extreme pressure performance of PAO 100 grease

The extreme pressure (EP) properties, such as pre-seizure and weld load of MWCNTs and LaF₃ blended PAO grease with varying concentrations of nanoadditives, are displayed in **Figure 7.5**. The pre-seizure and weld load for PAO grease was found to be 160 and 200 kgf, respectively. The addition of 0.025-0.075 wt.% doses of MWCNTs and 0.025- 0.1 wt.% LaF₃ nanoparticles in PAO grease were unable to impact EP properties. However, it

was noticed from **Figure 7.5** that PAO grease having 0.10-0.15 wt.% of MWCNTs and 0.15 wt.% of LaF₃ exhibited the enhancement in load carrying capacity of PAO grease. The pre-seizure load was increased from 160 to 200 kgf, and the weld load was augmented from 200 to 250 kgf. The results suggested that higher concentrations of nanoadditive in PAO grease are easier to deposit on friction surfaces to exert a self-repairing function. Therefore, resulting in the enhancement in EP property. In contrast, the nanoadditive might have been squeezed out from the interacting surfaces at lower concentrations due to the development of remarkably high Hertzian stress (~5.9 GPa corresponding to 200 kgf weld load) [69]. Therefore, nanoadditive did not contribute to the augmentation in the load-carrying capacity of the PAO grease.

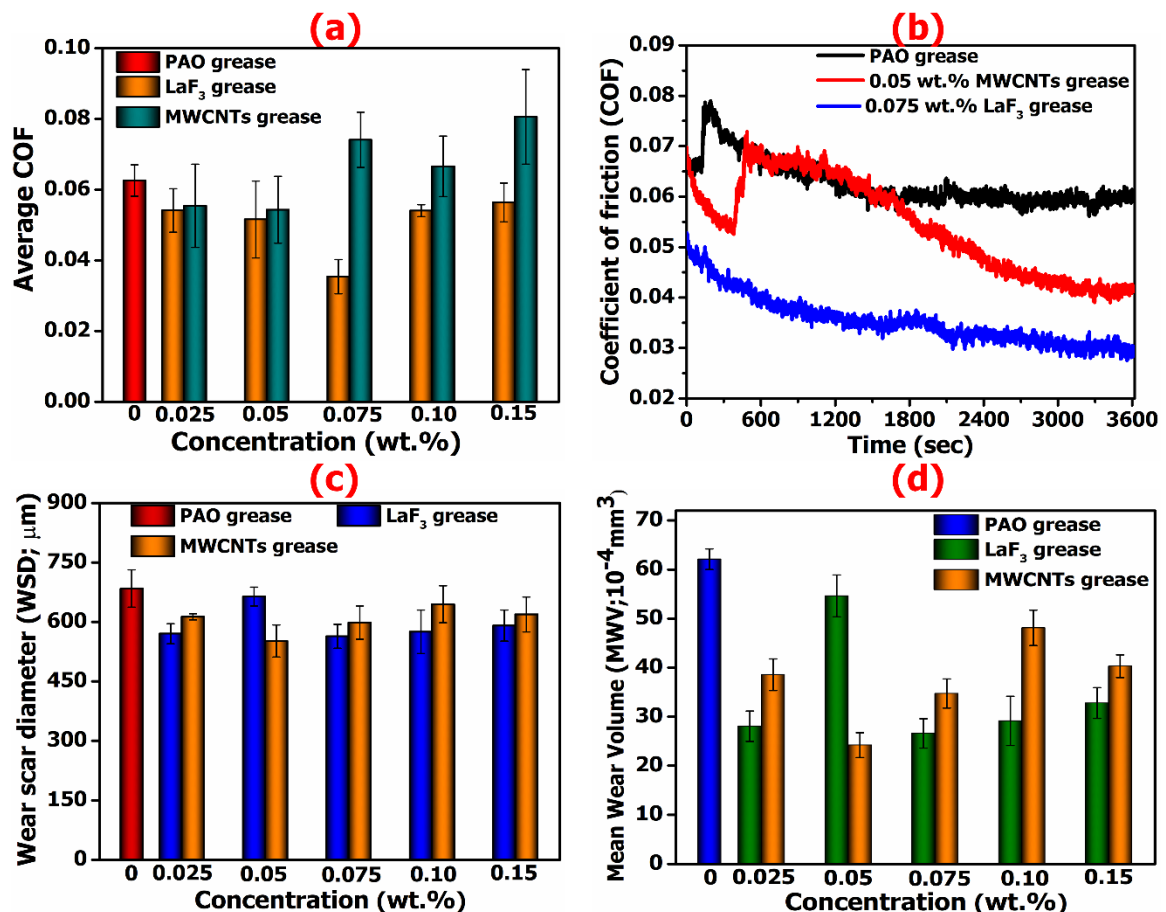


Figure 7.4: Variation in (a) average COF with variable concentration of MWCNTs and LaF₃ nanoparticles in PAO grease (b) COF as a function of test duration, and influence of varying concentrations of nanoadditive on (c) wear scar diameter and (d) the mean wear volume of worn surfaces. (Applied load: 392 N and test duration: 60 min)

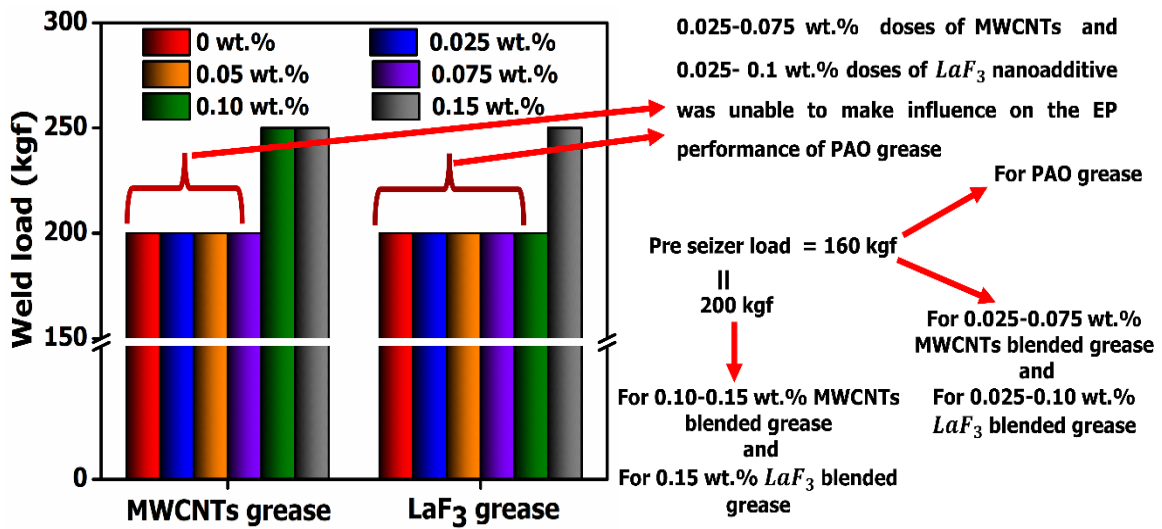


Figure 7.5: EP response of varied doses of MWCNTs and LaF_3 blended PAO grease

Table 7.1: Summary of frictional power loss at different concentrations of MWCNTs and LaF_3 nanoparticles

| Concentration (wt.%) | MWCNTs blended PAO grease | | LaF_3 blended PAO grease | |
|----------------------|---------------------------|---|----------------------------|---|
| | Power consumption (MJ) | Percentage reduction in power consumption | Power consumption (MJ) | Percentage reduction in power consumption |
| 0 | 49.79 | - | 49.79 | - |
| 0.025 | 44.12 | 11.40 | 43.06 | 13.52 |
| 0.05 | 43.21 | 13.22 | 41.05 | 17.56 |
| 0.075 | 58.95 | -18.38 | 28.16 | 43.46 |
| 0.1 | 53.01 | -6.44 | 43.01 | 13.63 |
| 0.15 | 64.11 | -28.75 | 44.84 | 9.94 |

7.4. Worn surface analysis

7.4.1. Worn surface analysis by SEM

Figure 7.6 depicts SEM micrographs of worn surfaces of steel balls at low and high magnifications. SEM images of the worn surfaces at low magnification (100X) give an idea about the WSD and overall wear characteristics. In contrast, higher magnification images at 1000X help to understand the nature of the wear mechanism. It can be observed from **Figures 7.6(a)-7.6(b)** that relatively larger wear scar along with the clear characteristics of deep and wide furrows and ploughing marks appeared along the sliding direction under the lubrication of PAO grease, indicating the possible sign of abrasive wear. This might be due to the continuous formation and decomposition of protective tribo-film resulting from the interaction of thickener molecules with the metal surface. The fibrous network of the thickener entraps the base oil via van der Waals and capillary interactions [175]. The thickener and base oil both contributed to the formation of a protective tribo-film. However, during the friction process, the temperature may rise due to collision of asperity or high Hertzian stress (~ 3.4 GPa), which causes the degradation of grease and bleeding of base oil from the fibrous structure. Furthermore, it was assumed that base oil and thickener molecules are generally squeezed out under high Hertzian stress and temperature [85]. Consequently, metal-to-metal contact occurred at the interface of rubbing surfaces, resulting in higher friction and wear (as displayed in **Figure 7.4**). It can be seen from **Figures 7.6(b)-7.4(c)** that the presence of 0.05 wt.% MWCNTs in PAO grease attenuated the magnitude of wear scar as well as the intensity of abrasive grooves. MWCNTs can easily penetrate and deposit in the grooves and valleys of the friction pairs and act as an effective mediator (i.e., solid lubricant), restricting the contact of friction pairs. The high thermal conductivity of MWCNTs also enables resistance to friction heat, lowering the surface temperature and minimizing the probability of adhesion between the rubbing

surfaces [141]. Therefore, MWCNTs tend to form thin, dry lubricant film covering the surface asperities and promoting smooth surfaces. The significantly smaller wear scar and smoothest surface with few light furrows were obtained when lubricated with 0.075 wt.% LaF₃ doped grease (**Figures 7.6(e)-7.4(f)**). This might be ascribed to the deposition and self-repairing function of LaF₃ on the mating surface. The extent of surface smoothness varied due to the difference in the contribution of LaF₃, PAO oil, and lithium soap (thickener) molecules towards film formation.

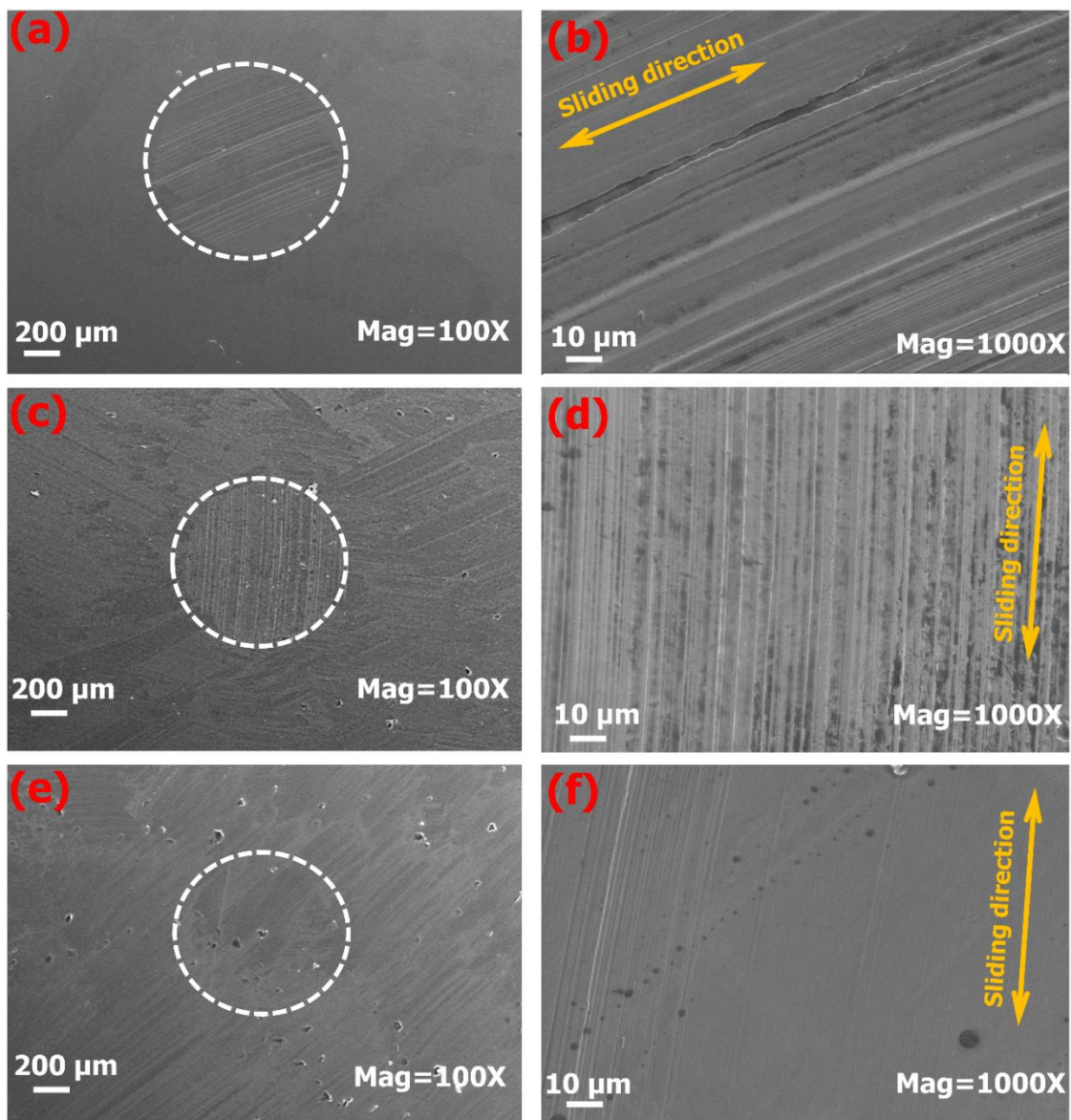


Figure 7.6: SEM micrographs of worn surfaces of steel balls lubricated with (a, b) PAO grease; (c, d) 0.05 wt.% MWCNTs doped grease; (e, f) 0.075 wt.% LaF₃ doped grease. (Applied load: 392 N and test duration: 60 min)

7.4.2. Surface topographic analysis of worn surfaces by SPM

The surface topography in the form of 2 D and 3 D micrographs of worn surfaces of worn steel balls lubricated by different grease formulations are displayed in **Figure 7.7**, and corresponding roughness values of worn surfaces are listed in Table 7.2. Figure 7.7(a) depicts the 2D view (deflection image) of worn surface lubricated by PAO grease, indicating irregular rough surface with deep scratches and grooves (i.e., non-uniform distribution of orange, red, green, and blue colour). The surface roughness (S_q) was estimated to be 443.4 nm. The 3D micrograph (**Figure 7.7(b)**) revealed the severity of abrasive wear on the worn surface. In contrast, MWCNTs blended grease (**Figures 7.7(c)-7.7(d)**) showed the shallower grooves with a relatively smooth surface than PAO grease, and the surface roughness was decreased to 307 nm. The smoothest surface with fewer furrows was observed when lubricated with LaF_3 blended grease (**Figures 7.7(e)-7.7(f)**). Furthermore, the 2D image (**Figure 7.7(e)**) featured the uniform green and blue colour distribution, signifying a low friction area. The physical attributes and very low hardness of LaF_3 nanoparticles enable them to enter and quick smear inside the contacts zone and form a beneficial protective film, resulting in lower friction and wear (**Figure 7.4**). Consequently, The surface roughness (S_q) value was undergone an enormous reduction (~83%), which can be seen explicitly in SEM micrographs (**Figures 7.6(e)-7.6(f)**).

Besides roughness, other amplitude parameters such as skewness (S_{sk}) and kurtosis (S_{ku}) also probed to predict surface performance better and are summarised in **Table 7.2**. The skewness (S_{sk}) is a measure of the asymmetry of the surface height distribution, and it is sensitive to occasional deep valleys or high peaks. For an asymmetric distribution of topography heights, the skewness may be negative if the distribution has more valleys or positive if the distribution has more peaks. The worn surface of the steel ball lubricated

with PAO grease and MWCNTs blended grease showed the negative skewness, indicating more valleys on the worn surface as shown in SPM micrographs (**Figure 7.7**). While worn surface lubricated with LaF₃ doped grease demonstrated the positive skewness, which inferred that LaF₃ nanoparticles were deposited in the valleys and produced relatively smooth surfaces with few peaks rather than valleys revealed by SPM micrographs. Kurtosis (S_{ku}) of the topography height distribution is always presented in conjunction with the skewness to describe the shape of the topography height distribution. It is the measure of the sharpness of the topography height distribution. A centrally distributed topography height distribution having a kurtosis value of higher than 3 ($S_{ku} > 3$) is called a leptokurtic surface, demonstrating a spiky surface (i.e., relatively many high peak and low valleys). In contrast, well-spread height distribution acquiring kurtosis value lower than 3 ($S_{ku} < 3$) is known as platykurtic surface, which features relatively few high peaks and low valleys [171]. Therefore, all worn surfaces of owing $S_{ku} < 3$ (as shown in **Table 7.2**) are platykurtic surfaces.

Bearing area ratio (BAR) curves for worn surfaces of steel balls lubricated with various grease formulations were also plotted to better conceptualise the peaks, valleys, and their respective distribution on worn surfaces. The BAR curves are arranged in **Figure 7.8**, and corresponding values of various morphological parameters ($S_k, S_{pk}, S_{vk}, S_{r1}, S_{r2}$) are listed in **Table 7.2**. **Figure 7.8(a)** depicts the representation of all symbols used in the BAR curve. The upper fragment of the BAR curve is denoted as reduced peak height (S_{pk}), which is generally worn out during the running-in period. The middle region is expressed as the core zone (S_k) that sustains the load during the stable period and affects the longevity of the components. The lower segment of the curve is called reduced valley depth (S_{vk}) which functions as a lubricant reservoir. The parameters S_{r1} and S_{r2} represent the percentage of bearing area ratio found in the limits of the core profile. It can be observed from **Figure 7.8**

and **Table 7.2** that MWCNTs and LaF₃ blended grease demonstrated a significant reduction in S_k , S_{pk} , S_{vk} , S_{r1} and minimal increment in S_{r2} compared to PAO grease. This indicated that the peaks on the worn surface were polished off, and valleys were filled by nanoadditives, which led to flattening the middle region of its BAR curve. As a result, surfaces with comparable smoothness were acquired as displayed in SEM and SPM images (**Figure 7.6** and **Figure 7.7**). The increment in S_{r2} implies the good retention capacity of lubricating grease in the micro valleys of rubbing surfaces. The worn surface lubricated with LaF₃ doped grease showed the lowest value of S_k , indicating the flattest curve among all BAR curves.

Hybrid parameters are also important in surface engineering because these are concerned with both height (amplitude) and plane direction (spacing). These parameters are derived from mathematical models that interpret spatial and vertical characteristics of the surface simultaneously and are essential for quantifying wear in tribological tests [176]. The hybrid parameter may be affected by any changes in either amplitude or spacing. This study investigates, the two-hybrid parameters, i.e., mean slope of profile (Δ_a) and RMS slope of profile (Δ_q) are investigated, as shown in Table 7.2. A higher value may signify a peaky surface, whereas a low value may denote a smoother surface. The sampling interval significantly influences the RMS slope (Δ_q). The worn surface lubricated by LaF₃ doped grease showed the lowest value of both hybrid parameters, implying the smoothest worn surface among all grease formulations, which is also corroborated by SEM and SPM results (**Figure 7.6** and **Figure 7.7**).

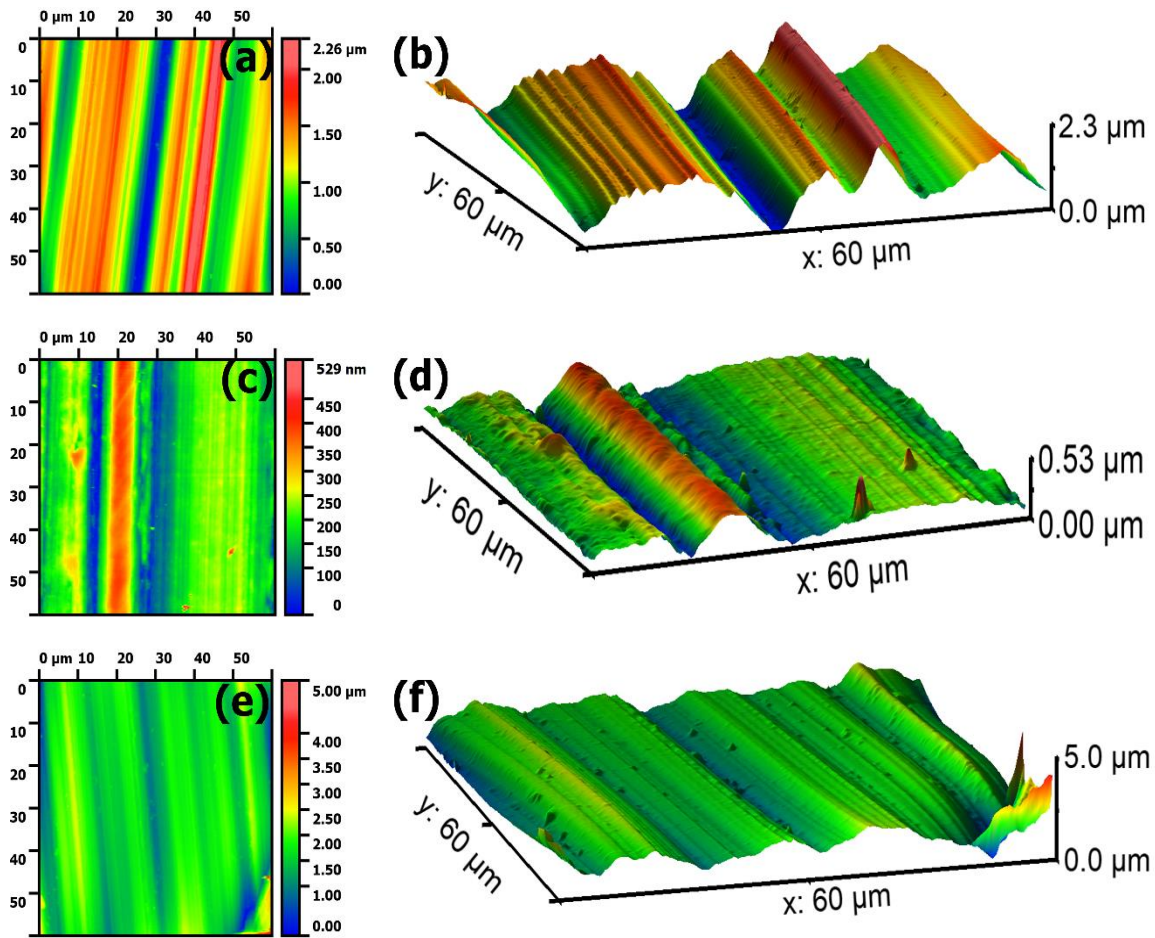


Figure 7.7: Topographic micrographs of worn surfaces of steel balls lubricated with (a, b) PAO grease; (c, d) 0.05 wt.% MWCNTs doped grease; (e, f) 0.075 wt.% LaF₃ doped grease. (Note: a, c, and e: top view (2D) and b, d, and f: three-dimensional (3D) view of worn surfaces). (Applied load: 392 N and test duration: 60 min)

Table 7.2: Surface roughness parameter of worn steel balls tested with various grease formulations

| Lubricant composition | Surface roughness | | Amplitude parameter | | Morphological parameter | | | | | Hybrid parameter | |
|--|-------------------|---------------|---------------------|----------|-------------------------|------------------|------------------|-----------------|-----------------|------------------|------------|
| | S_a (nm) | S_q (nm) | S_{sk} | S_{ku} | S_k (nm) | S_{pk} (nm) | S_{vk} (nm) | S_{r1} (%) | S_{r2} (%) | Δ_a | Δ_q |
| PAO grease | 355.2 | 443.4 | -0.1951 | 0.04735 | 400.3 | 86.7 | 101.6 | 7.4 | 89.07 | 0.1468 | 0.1872 |
| 0.05 wt.% MWCNTs grease | 249.9 | 307.5 | -0.1407 | 0.4712 | 375.4 | 12.5 | 69.3 | 6.4 | 91.6 | 0.1334 | 0.1696 |
| 0.075 wt.% LaF₃ grease | 58.92 | 76.34 | 0.2558 | 0.3041 | 66.3 | 15.9 | 13.1 | 4.9 | 90.8 | 0.0264 | 0.0387 |

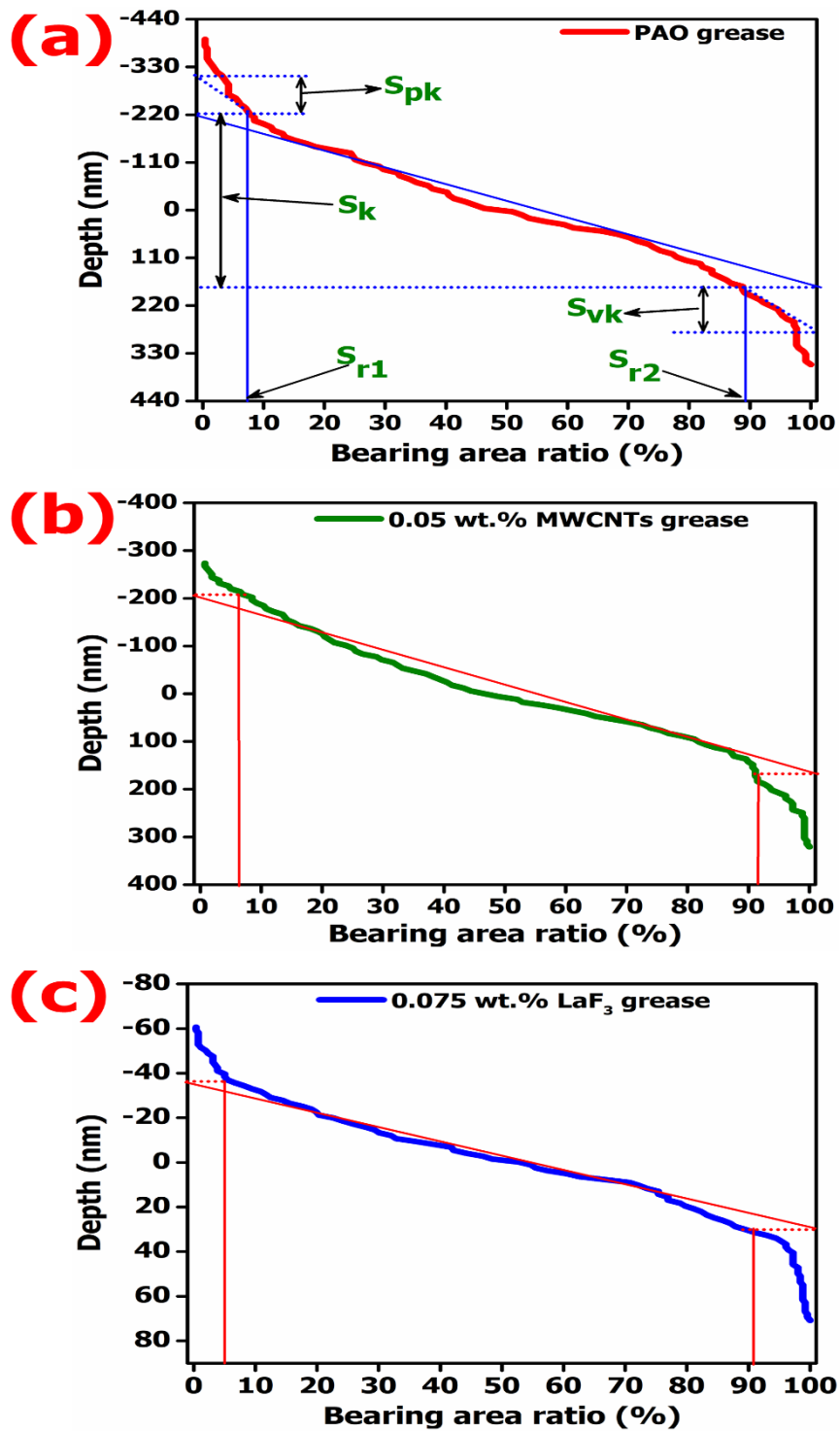


Figure 7.8: Bearing area ratio curves of steel balls lubricated with different grease compositions. (Applied load: 392 N and test duration: 60 min)

7.4.3. EDS analysis of worn Surfaces

The chemical composition on worn surfaces of steel balls lubricated by various grease formulations was probed using EDS, and the results are shown in **Figure 7.9**. It can be

observed that lithium from grease thickener was not detected on all worn surfaces because EDS systems can detect only elements with the atomic number $Z \geq 4$. The worn surface lubricated by MWCNTs blended grease (**Figures 7.9(c)-7.9(d)**) exhibited the highest atomic concentration of C (59.8 %), which can be ascribed to the physical adsorption of MWCNTs on the friction surface, leading to the formation of stable tribo-film during friction process. On the contrary, F and La, along with Fe, C, Cr, O elements, were identified on the worn surfaces lubricated by LaF₃ doped grease (**Figures 7.9(e)-7.9(f)**), which illustrates that LaF₃ nanoparticles may accumulate in the nano grooves of rubbing surfaces to form tribo-film. Consequently, preventing direct metal-to-metal contact leads to reduce in friction and wear (**Figure 7.4**). The presence of O on all worn surfaces could be attributed to oxidative events during the tribo-tests.

7.4.4. XPS analysis of worn surfaces

The EDS results can not accurately reflect the chemical composition of worn surfaces due to the limited sensitivity of EDS, especially light elements such as O and C. Therefore, XPS was used to identify the chemical states of the individual elements of the tribo-film formed on worn surfaces. The XPS analysis results are presented in **Figures 7.10-7.12**. XPS survey spectra (**Figure 7.10**) exhibited the presence of C 1s, Fe 2p, O 1s, and Li 1s on all worn surfaces, indicating the formation of the lubricating thin layer over the interface of steel balls based on PAO grease. The Li 1s peak on all surfaces is attributed to the lithium soap, which is the major constituent of all grease samples. The presence of O 1s revealed the thermo-oxidation of grease and oxides formation on the worn surfaces.

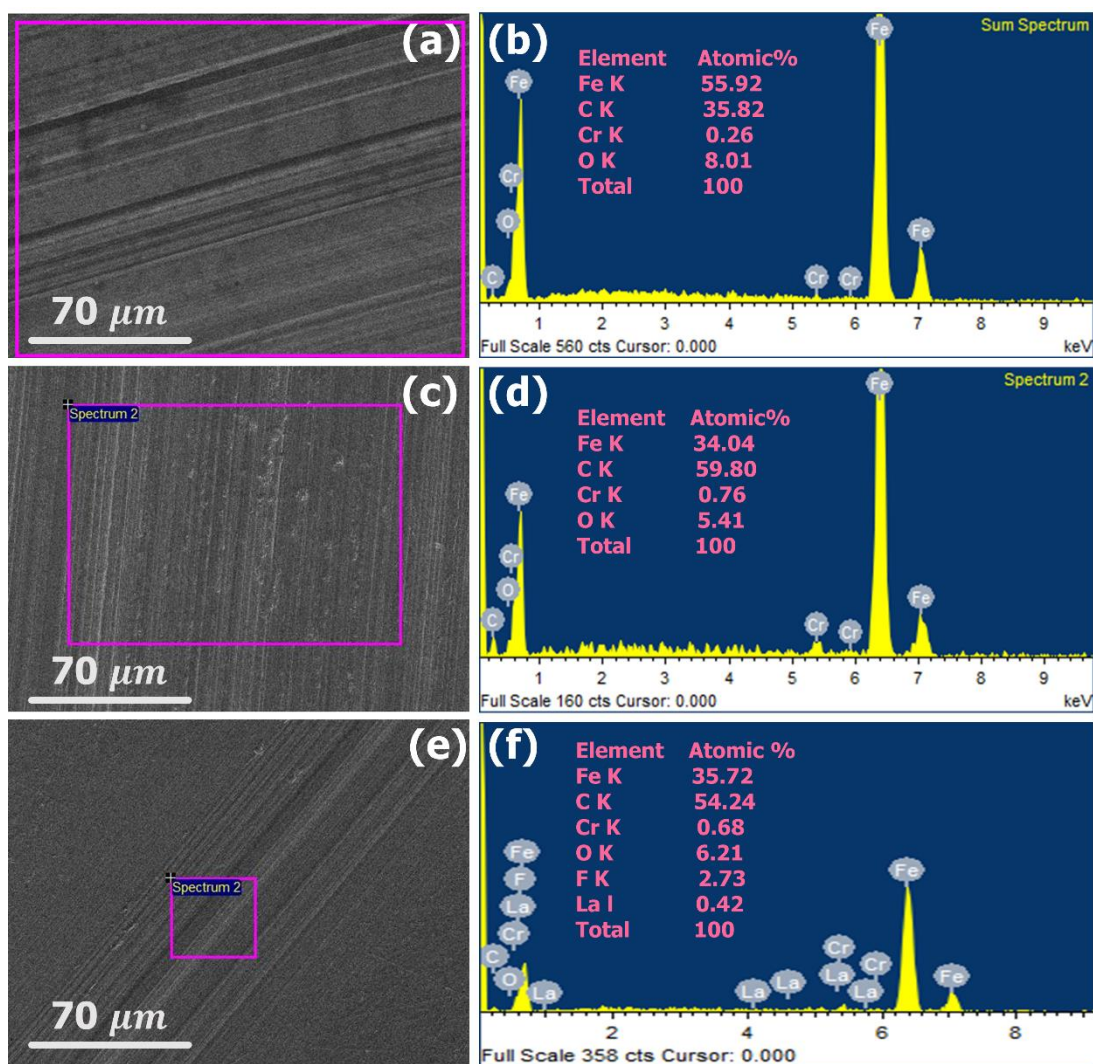


Figure 7.9: EDS spectrum of worn scars of steel balls lubricated by (a, b) PAO grease; (c, d) 0.05 wt.% MWCNTs doped grease; (e, f) 0.075 wt.% LaF₃ doped grease. (Applied load: 392 N and test duration: 60 min)

The high-resolution spectra of C 1s of worn surface lubricated with PAO grease (**Figure 7.11(a)**) exhibit three peaks with binding energies 285.45, 285.98, and 288.84 eV. The peak with binding energy 285.45 eV could be ascribed to C-C bonds. The other peaks at 285.98 and 288.84 are assigned to C-O and O-C=O bonds [146,147]. C-O bonds are mainly ascribed to organic compounds. For the PAO grease, C-C bond corresponds to the contaminated carbon. While for the MWCNTs blended grease, the C-C bond is mainly ascribed to the contaminated carbon and the carbon from MWCNTs. The Fe 2p spectra (Figure 7.11(b)) can be deconvoluted into four peaks appeared at 710.82 eV, 712.18 eV,

724.34 eV, and 726.45 eV. The Fe 2p peaks at 710.82 eV and 724.34 eV together confirmed the presence of Fe₂O₃. The peak that appeared at 712.18 eV is credited to FeOOH [177]. The core-level spectra of O 1s reveal the four peaks, as shown in Figure 7.11(c). The O 1s binding energies at 530.29 and 531.84 eV are assigned to the Fe-O bond and FeOOH, respectively [166]. The XPS spectra of C 1s, Fe 2p, and O 1s of worn surfaces lubricated with MWCNTs grease (**Figures 7.11(d)-7.11(f)**) demonstrated a negligible difference in peaks compared to surface lubricated with PAO grease (**Figures 7.11(a)-7.11(c)**). In contrast, it is evident in XPS survey spectra (**Figure 7.10**) that the worn surface lubricated with MWCNTs grease had the high intense C1s peak (i.e., the highest carbon content). On the other hand, the worn surface showed the lowest intensity of O1s peak (lowest O content and lowest oxidation). Furthermore, deconvoluted spectra of C 1s at 285.06 eV (C-C bonds) in **Figure 7.11(d)** demonstrated a higher peak intensity than worn surface lubricated by PAO grease. Thus, it may be inferred that tribo-films composed of Fe₂O₃, FeOOH, and organic compounds were formed on the worn surfaces under the PAO grease lubrication. While in the case of MWCNTs blended grease, the tribo-films mainly consist of Fe₂O₃, FeOOH, MWCNTs, and organic compounds.

The deconvoluted XPS spectra of typical elements on worn surface lubricated with LaF₃ blended grease are depicted in **Figure 7.12**. Two weak Fe 2p_{3/2} peaks appeared at 710.8 eV and 711.75 eV. The Fe 2p at 710.8 eV, associated with the O 1s at 530.28 eV, can be identified as Fe₂O₃. While Fe 2p peak at 711.75 eV, in combination with the Fe 1s peak at 687.3 eV, can be assigned to FeF₃ [79]. The binding energy of La 3d at 837.5 eV in association with the O 1s peak at 528.56 eV indicates that La₂O₃ exists on the worn surface [178]. Besides, the La 3d peak appears at 837.5 eV, and the F 1s peak appears at 684.88 eV, which indicates that LaF₃ exists on the worn surface of the steel balls [78,179]. The above XPS results illustrated the tribo-chemical reaction that occurred at the interface of

tribo-pairs during the friction process under the lubrication of LaF₃ doped grease. As a result, a stable lubricating film consisting of the deposition layer of LaF₃ nanoparticles and the reaction layer composed of Fe₂O₃, FeF₃, and La₂O₃ was formed between the rubbing surface, resulting in a significant reduction in friction and wear (as shown in **Figure 7.4**). Furthermore, LaF₃ nanoparticles can chemically adsorb on sliding surfaces to form lubricating films with good tribological performance. Hence, LaF₃ nanoparticles play an important role in improving the friction reduction and anti-wear properties of PAO grease, which is closely related to the deposition of surface-modified LaF₃ nanoparticles on worn surfaces and the self-healing action of the nanoparticles for the micro-defects present on surfaces [78].

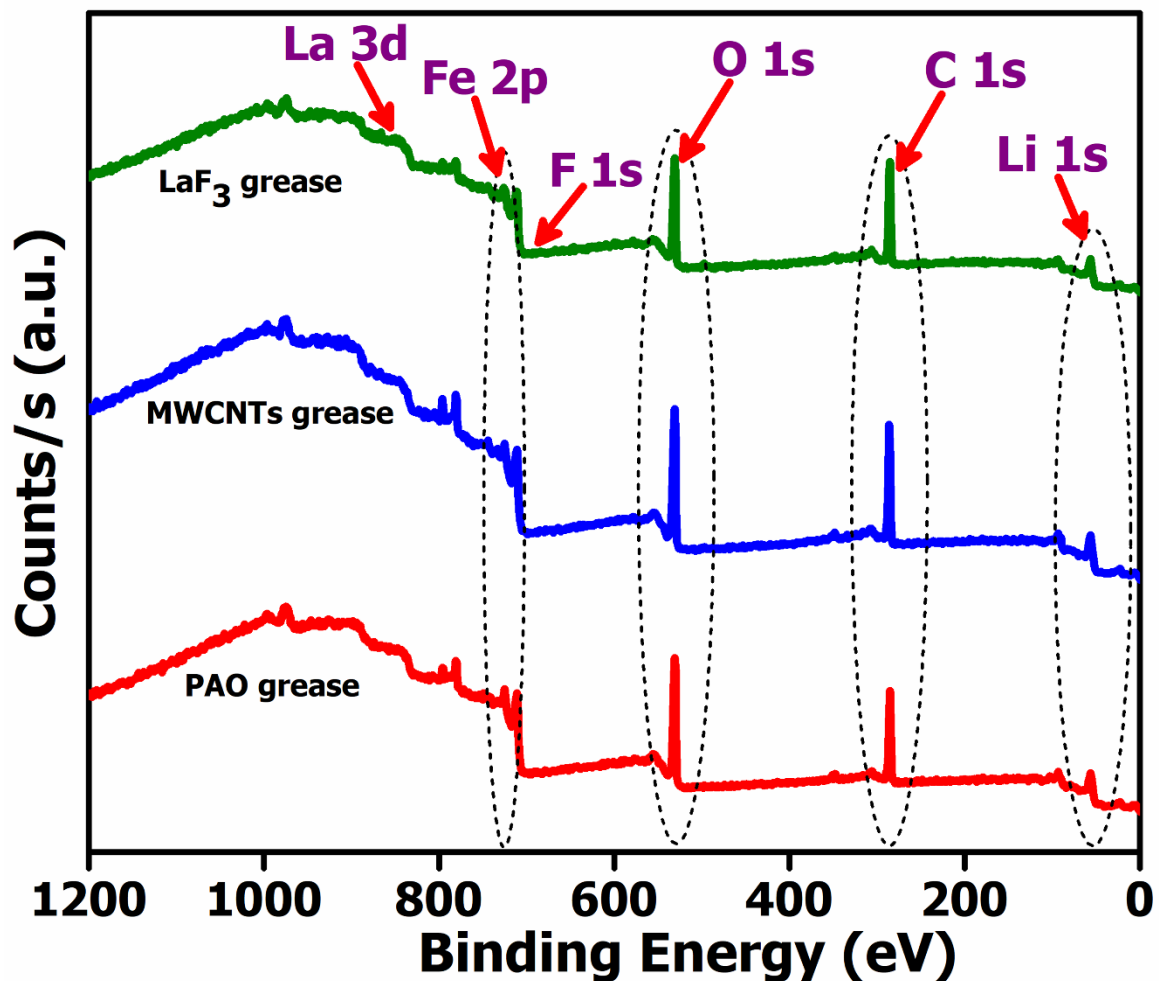


Figure 7.10: XPS of worn surface of steel ball lubricated with various grease formulations. (Applied load: 392 N and test duration: 60 min)

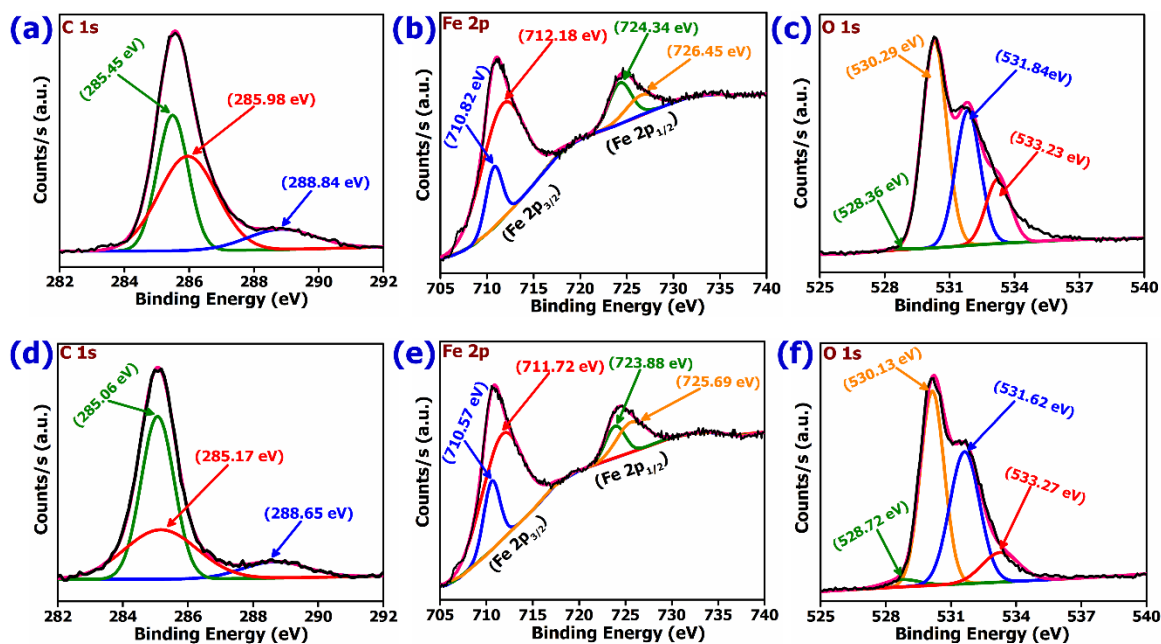


Figure 7.11: High-resolution XPS spectra showing typical elements on the worn surface of steel balls lubricated with (a, b, and c) PAO grease and (d) MWCNTs doped grease. (Applied load: 392 N and test duration: 60 min)

7.5. Summary of the chapter

The grease was formulated with PAO 100 as base oil, and the 12–lithium hydroxystearate was used as a thickener. Further, MWCNTs and LaF₃ nanoparticles were used as nanoadditives and blended in PAO grease in variable concentrations. The tribological performance of PAO grease with and without nanoadditives was evaluated using a four-ball tester. The experimental results revealed that PAO grease in the presence of LaF₃ nanoparticles performed superior among all PAO grease samples.

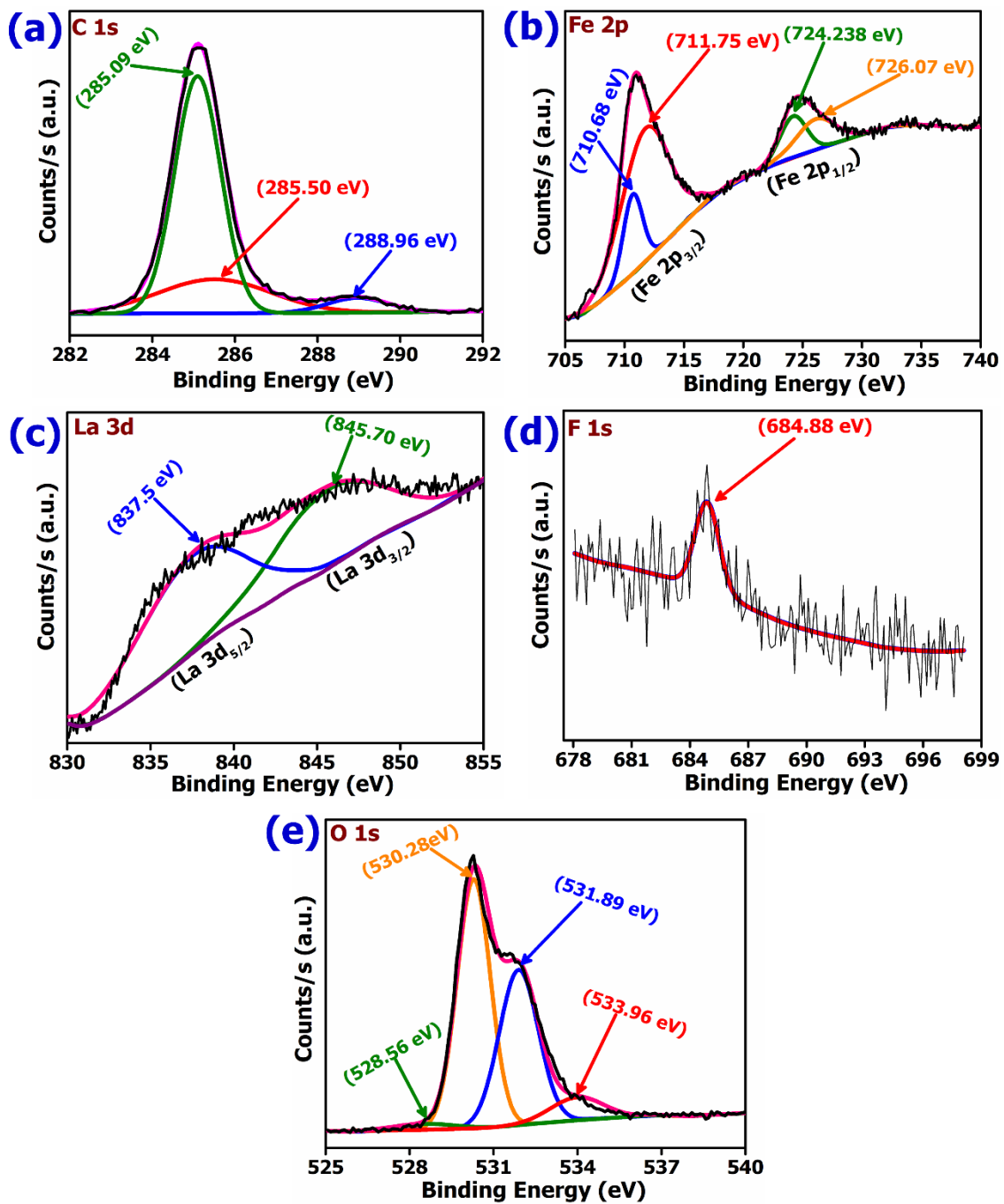


Figure 7.12: High-resolution XPS spectra showing typical elements on the worn surface of steel balls lubricated with LaF₃ doped grease. (Applied load: 392 N and test duration: 60 min)